

Synthesis and Structure of Multicomponent Crystals of Fullerenes and Metal Tetraarylporphyrins

Dmitri V. Konarev,[†] Andrey Yu. Kovalevsky,[‡] Xue Li,[‡] Ivan S. Neretin,[§] Alexey L. Litvinov,[†] Natal'ya V. Drichko,^{||} Yuri L. Slovokhotov,[§] Philip Coppens,[‡] and Rimma N. Lyubovskaya^{*†}

Institute of Problems of Chemical Physics RAS, Chernogolovka, Moscow Region 142432, Russia, Crystallography Laboratory, Department of Chemistry, State University of New York at Buffalo, Buffalo, New York 14260, Institute of Organoelement Compounds RAS, 28 Vavilov St., 117334 Moscow, Russia, and A. F. Ioffe Physical-Technical Institute, St. Petersburg 194021, Russia

Received December 27, 2001

The preparation of fullerene complexes with metal tetraarylporphyrins in the presence of excess ferrocene (Cp₂Fe) results in the formation of new solvent-free and multicomponent molecular crystals. New isomorphous complexes of C₆₀ with PyZnTPP (ZnTPP ≡ zinc 5,10,15,20-tetraphenyl-21*H*,23*H*-porphyrinate) and PyCoTPP (CoTPP ≡ cobalt(II) 5,10,15,20-tetraphenyl-21*H*,23*H*-porphyrinate) containing Cp₂Fe and the isostructural C₇₀ complex with PyZnTPP have been prepared. The crystal structures of the new layered C₆₀ complexes CoTMPP·C₆₀ (obtained in the presence of Cp₂Fe) and CoTMPP·2C₆₀·3C₇H₈ (obtained in the absence of Cp₂Fe) have been described (CoTMPP ≡ cobalt(II) 5,10,15,20-tetrakis(*p*-methoxyphenyl)-21*H*,23*H*-porphyrinate). Cobalt atoms of the PyCoTPP and CoTMPP molecules are weakly coordinated to C₆₀ with Co···C(C₆₀) distances in the 2.64–2.82 Å range, whereas zinc atoms of PyZnTPP, as well as cobalt atoms of the CoTMPP molecules in the solvent-free phase, form only van der Waals contacts with fullerenes. Different packing arrangements in the crystals of fullerene–porphyrin complexes have been discussed.

Introduction

Molecular complexes of fullerenes¹ with organic and organometallic donors have recently attracted much attention. More than 100 complexes^{2–5} with tetrachalcogenafulvalenes,^{5–8} aromatic hydrocarbons,^{5,9} amines,^{5,10} metallocenes,^{2,3,5,11,12} porphyrins and metalloporphyrins,^{13–18} and other potentially

donor molecules^{19,20} have been obtained and characterized. Most of these complexes have a neutral ground state, but further modification can result in the formation of charged species with conducting and magnetic properties.

Fullerenes can form two-component complexes with S₈, Cp₂Fe, ET, TP, DPA,³⁴ and others^{3,5,6,11} and three- or four-

* Author to whom correspondence should be addressed. E-mail: lyurn@icp.ac.ru.

[†] Institute of Problems of Chemical Physics, Russian Academy of Sciences.

[‡] State University of New York at Buffalo.

[§] Institute of Organoelement Compounds, Russian Academy of Sciences.

^{||} A. F. Ioffe Physical-Technical Institute.

- (1) Kroto, H. W.; Heath, J. R.; O'Brien, S. C.; Curl, R. F.; Smalley, R. E. *Nature* **1985**, *318*, 162.
- (2) Balch, A. L.; Olmstead, M. M. *Chem. Rev.* **1998**, *98*, 2123.
- (3) Konarev, D. V.; Lyubovskaya, R. N. *Russ. Chem. Rev.* **1999**, *68* (1), 19.
- (4) Hardie, M. J.; Raston, C. L. *J. Chem. Soc., Chem. Commun.* **1999**, 1153.
- (5) Konarev, D. V.; Lyubovskaya, R. N.; Drichko, N. V.; Yudanov, E. I.; Shul'ga, Yu. M.; Litvinov, A. L.; Semkin, V. N.; Tarasov, B. P. *J. Mater. Chem.* **2000**, 803.
- (6) Izuoka, A.; Tachikawa, T.; Sugawara, T.; Suzuki, Y.; Konno, M.; Saito, Y.; Shinohara, H. *J. Chem. Soc., Chem. Commun.* **1992**, 1472.
- (7) Saito, G.; Teramoto, T.; Otsuka, A.; Sugita, Y.; Ban, T.; Kusunoki, M.; Sakaguchi, K. *Synth. Met.* **1994**, *64*, 359.
- (8) Konarev, D. V.; Zubavichus, Y. V.; Slovokhotov, Yu. L.; Shul'ga, Yu. M.; Semkin, V. N.; Drichko, N. V.; Lyubovskaya, R. N. *Synth. Met.* **1998**, *92*, 1.

- (9) Konarev, D. V.; Valeev, E. F.; Slovokhotov, Yu. L.; Shul'ga, Yu. M.; Lyubovskaya, R. N. *J. Chem. Res., Synop.* **1997**, 442.
- (10) Stephens, P. W.; Cox, D.; Lauher, J. W.; Mihaly, L.; Wiley, J. B.; Allemand, P.-M.; Hirsh, A.; Holzer, K.; Li, Q.; Tompson, J. D.; Wudl, F. *Nature (London)* **1992**, *355*, 331.
- (11) Crane, J. D.; Hitchcock, P. B.; Kroto, H. W.; Taylor, R.; Walton, R. M. *J. Chem. Soc., Chem. Commun.* **1992**, 1764.
- (12) Wan, W. C.; Liu, X.; Sweeney, G. M.; Broderick, W. E. *J. Am. Chem. Soc.* **1995**, *117*, 9580.
- (13) Olmstead, M. M.; Costa, D. A.; Maitra, K.; Noll, B. C.; Phillips, S. L.; Van Calcar, P. M.; Balch, A. L. *J. Am. Chem. Soc.* **1999**, *121*, 7090.
- (14) Boyd, P. D. W.; Hodgson, M. C.; Rickard, C. E. F.; Oliver, A. G.; Chaker, L.; Brothers, P. J.; Bolskar, R. D.; Tham, F. S.; Reed, C. A. *J. Am. Chem. Soc.* **1999**, *121*, 10487.
- (15) Konarev, D. V.; Neretin, I. S.; Slovokhotov, Yu. L.; Yudanov, E. I.; Drichko, N. V.; Shul'ga, Yu. M.; Tarasov, B. P.; Gumanov, L. L.; Batsanov, A. S.; Howard, J. A. K.; Lyubovskaya, R. N. *Chem. Eur. J.* **2001**, *7*, 2605.
- (16) Ishii, T.; Aizawa, N.; Yamashita, M.; Matsuzaka, H.; Kodama, T.; Kikuchi, K.; Ikemoto, I.; Iwasa, Y. *J. Chem. Soc., Dalton Trans.* **2000**, 4407.
- (17) Evans, D. R.; P. Fackler, N. L.; Xie, Z.; Rickard, C. E. F.; Boyd, P. D. W.; Reed, C. A. *J. Am. Chem. Soc.* **1999**, *121*, 8466.

component complexes containing solvent molecules.^{3,5,7–9,13–20} Replacing some of the solvent molecules for another strong donor or acceptor ones, one can modify electronic states of the fullerene or donor component, respectively.^{21,22} For example, the doping of fullerene complexes with donors D by alkali metals M results in the formation of three-component solids $D \cdot (C_{60}^- \cdot nM^+)$ in which a superconducting phase is observed at T_c up to 26 K.²¹ Exposure of neutral C_{60} complexes with TMDTDM-TTF, DBTTF, and TPDP³⁴ to iodine vapor results in the substitution of the solvent molecule by iodine, while the organic component is oxidized, thus forming donor radical cations and I_n^- anions.^{22a} Diffusion of iodine into a solution containing C_{60} and ET³⁴ yields single crystals of $(ET^{\bullet+} \cdot I_3^-)C_{60}$,^{22b} in which the layers of the $ET^{\bullet+} \cdot I_3^-$ radical cation salt alternate with those of the neutral C_{60} molecules.

To introduce potentially donor molecules in a neutral supramolecular environment, we prepared fullerene complexes with metal tetraarylporphyrins in the presence of an excess of ferrocene. We report here the preparation of mixed crystals of fullerenes with Zn and Co tetraarylporphyrinates in the presence and absence of Cp_2Fe . For the first time fullerene complexes with two donor counterparts,³⁵ namely, metalloporphyrin and the Cp_2Fe molecules, were obtained. The second donor component, e.g., Cp_2Fe , occupies a position close to that of solvent trichloroethylene molecule in the crystal structures of the quasi-isomorphous series $2PyZnTPP \cdot C_{60} \cdot Cp_2Fe \cdot C_7H_8$, $2PyCoTPP \cdot C_{60} \cdot Cp_2Fe \cdot C_7H_8$, and $2PyZnTPP \cdot C_{70} \cdot C_2HCl_3 \cdot C_7H_8$. The crystal structures of the two other complexes of C_{60} with CoTMPP, viz. solvent-free CoTMPP· C_{60} (crystallized in a large excess of Cp_2Fe) and solvated CoTMPP· $2C_{60} \cdot 3C_7H_8$ (obtained in the absence of Cp_2Fe) are also reported.

Experimental Section

General. IR spectra of the samples (KBr pellets, 1:400) were recorded on a Perkin-Elmer 1725X spectrophotometer in the 400–

7000 cm^{-1} range. Electronic absorption spectra were measured on a Perkin-Elmer Lambda 19 UV–vis–NIR spectrophotometer in the 220–3000 nm range (KBr pellets, 1:2000).

Materials. All chemicals were purchased from Aldrich and used without further purification. Liquids were dried by distillation under argon over Na/benzophenone for benzene and toluene, P_2O_5 for trichloroethylene (C_2HCl_3), and KOH for pyridine. The solvents were stored under argon.

Syntheses. All the complexes were obtained by evaporation of solutions of fullerenes and corresponding metalloporphyrins under argon during 5–10 days. For the preparation of pyridine-containing complexes, the solvent was evaporated in the presence of pyridine vapor (10 mL of pyridine was loaded into a box to be evaporated in a separate glass). This method was used to obtain $2PyCoTPP \cdot C_{60} \cdot Cp_2Fe \cdot C_7H_8$ (**1**) and $2PyZnTPP \cdot C_{60} \cdot Cp_2Fe \cdot C_7H_8$ (**2**) from the toluene solution (30 mL) containing CoTPP or ZnTPP (36 mg, 0.056 mmol), C_{60} (20 mg, 0.033 mmol), and Cp_2Fe (52 mg, 0.28 mmol) at a 2:1:10 molar ratio. The solvent was decanted from the crystals of **1** and **2** before Cp_2Fe precipitated. Then the crystals were washed with dry acetone (50–60% yield).

$2PyZnTPP \cdot C_{70} \cdot C_2HCl_3 \cdot C_7H_8$ (**3**) was prepared by the same method from a toluene/trichloroethylene (1:9) solution (3/27 mL) containing ZnTPP (18 mg, 0.056 mmol) and C_{60} (20 mg, 0.028 mmol) at a 2:1 molar ratio. The solvent was decanted from the crystals of **3**, which were then washed with dry acetone (60–80% yield).

CoTMPP· C_{60} (**4**) was obtained by evaporation of the toluene solution (30 mL) containing CoTMPP (22 mg, 0.028 mmol), C_{60} (20 mg, 0.028 mmol), and Cp_2Fe (52 mg, 0.28 mmol) at a 1:1:10 molar ratio. The solvent was decanted from the crystals, which were then washed with dry acetone (60% yield).

CoTMPP· $2C_{60} \cdot 3C_7H_8$ (**5**) was prepared by evaporation of the toluene solution (30 mL) containing CoTMPP (22 mg, 0.028 mmol) and C_{60} (20 mg, 0.028 mmol) at a 1:1 molar ratio. The crystals of **1–5** are black prisms whose elemental composition was determined during X-ray analysis.

Crystal Structure Determination. Crystallographic information for **1–5** is summarized in Table 1. X-ray diffraction data for **1**, **4**, and **5** were collected at 90 K on a Bruker SMART diffractometer installed at a rotating anode generator (monochromatized Mo $K\alpha$ radiation, $\lambda = 0.71073 \text{ \AA}$), while data for **2** and **3** were collected at 110 K on a Bruker SMART diffractometer with a sealed X-ray tube (monochromatized Mo $K\alpha$ radiation). In all cases a series of ω scans with a 0.3° frame width were collected (six scans with different φ angles for **1**, **4**, and **5**, three scans for **2** and **3**). Reflection intensities were integrated using the SAINT program.²³

The SHELXTL program package²⁴ was used for structure solution and refinement; the latter was performed by full-matrix least squares on F^2 using all data. The ordered non-hydrogen atoms were refined anisotropically, with the hydrogen atoms (partially revealed in the difference Fourier maps) “riding” in idealized positions. Certain groups of atoms, specifically the carbon atoms of Cp_2Fe , disordered carbons of C_{60} and toluene in **2**, and C_{70} and solvent molecules in **3**, were refined isotropically. For the C_{70} molecule in **3** all the C–C bonds equivalent under D_{5h} symmetry were constrained to be equal.

- (18) (a) Stevenson, S.; Rice, G.; Glass, T.; Harich, K.; Cromer, F.; Jordan, M. R.; Craft, J.; Hadju, E.; Bible, R.; Olmstead, M. M.; Maitra, K.; Fisher, A. J.; Balch, A. L.; Dorn, H. C. *Nature* **1999**, *401*, 55. (b) Olmstead, M. M.; Bettencourt-Dias, A.; Duchamp, J. C.; Stevenson, S.; Dorn, H. C.; Balch, A. L. *J. Am. Chem. Soc.* **2000**, *122*, 12220. (c) Olmstead, M. M.; Bettencourt-Dias, A.; Duchamp, J. C.; Stevenson, S.; Marciu, D.; Dorn, H. C.; Balch, A. L. *Angew. Chem., Int. Ed.* **2001**, *40*, 1223.
- (19) (a) Hochmuth, D. H.; Michel, S. L. J.; White, A. J. P.; Williams, D. J.; Barrett, A. G. M.; Hoffman, B. M. *Eur. J. Inorg. Chem.* **2000**, 593. (b) Eichhorn, D. M.; Yang, S.; Jarrell, W.; Baumann, T. F.; Beall, L. S.; White, A. J. P.; Williams, D. J.; Barrett, A. G. M.; Hoffman, B. M. *J. Chem. Soc., Chem. Commun.* **1995**, 1703.
- (20) (a) Croucher, P. D.; Marshall, J. M. E.; Nichols, P. J.; Raston, C. L. *J. Chem. Soc., Chem. Commun.* **1999**, 193. (b) Croucher, P. D.; Nichols, P. J.; Raston, C. L. *J. Chem. Soc., Dalton Trans.* **1999**, 279. (c) Andrews, P. C.; Atwood, J. L.; Barbour, L. J.; Croucher, P. D.; Nichols, P. J.; Smith, N. O.; Skelton, B. W.; White, A. H.; Raston, C. L. *J. Chem. Soc., Dalton Trans.* **1999**, 2927. (d) Andrews, P. C.; Atwood, J. L.; Barbour, L. J.; Nichols, P. J.; Raston, C. L. *Chem. Eur. J.* **1998**, *4*, 1384.
- (21) (a) Otsuka, A.; Saito, G.; Teramoto, T.; Sugita, Y.; Ban, T.; Zakhidov, A. A.; Yakushi, K. *Mol. Cryst., Liq. Cryst.* **1996**, *284*, 345. (b) Otsuka, A.; Saito, G.; Hirate, S.; Pac, S.; Ishida, T.; Zakhidov, A. A.; Yakushi, K. *Mater. Res. Soc. Symp. Proc.* **1998**, *488*, 495.
- (22) (a) Lyubovskaya, R. N.; Konarev, D. V.; Yudanov, E. I.; Roschupkina, O. S.; Shul'ga, Yu. M.; Semkin, V. N.; Graja, A. *Synth. Met.* **1997**, *84*, 741. (b) Konarev, D. V.; Kovalevsky, A. Yu.; Coppens, P.; Lyubovskaya, R. N. *J. Chem. Soc., Chem. Commun.* **2000**, 2357.

- (23) SMART and SAINT, Area detector control and integration software, Version 6.01; Bruker Analytical X-ray Systems: Madison, WI, 1999.
- (24) SHELXTL, An integrated system for solving, refining and displaying crystal structures from diffraction data, Version 5.10; Bruker Analytical X-ray Systems: Madison, WI, 1997.

Table 1. Crystal Data for 1–5

	1	2	3	4	5
formula	2PyCoTPP·C ₆₀ ·Cp ₂ Fe·C ₇ H ₈	2PyZnTPP·C ₆₀ ·Cp ₂ Fe·C ₇ H ₈	2PyZnTPP·C ₇₀ ·C ₂ HCl ₃ ·C ₇ H ₈	CoTMPP·C ₆₀	CoTMPP·2C ₆₀ ·3C ₇ H ₈
<i>M_r</i> , g·mol ⁻¹	2499.22	2512.34	2573.5	1512.34	1250.64
crystal shape	black prisms	black prisms	black prisms	black prisms	black prisms
crystal system	monoclinic	monoclinic	monoclinic	triclinic	monoclinic
space group	<i>C2/c</i>	<i>C2/c</i>	<i>C2/c</i>	<i>P1</i>	<i>P2₁/c</i>
<i>a</i> , Å	30.5233(4)	30.797(2)	30.763(3)	13.1109(7)	13.984(1)
<i>b</i> , Å	19.5925(2)	19.532(2)	19.825(2)	15.3467(8)	21.388(2)
<i>c</i> , Å	19.2515(2)	19.312(1)	20.036(2)	16.4652(8)	18.178(2)
α, deg	90	90	90	90.617(1)	90
β, deg	92.067(1)	91.861(2)	92.250(2)	110.376(1)	96.586(2)
γ, deg	90	90	90	96.720(1)	90
<i>V</i> , Å ³	11 505.4(2)	11 611(1)	12 210(2)	3 079.6(3)	5 401.0(9)
<i>Z</i>	4	4	4	2	4
ρ _{calc} , g/cm ³	1.433	1.434	1.400	1.631	1.538
μ, mm ⁻¹	0.48	0.48	0.49	0.36	0.24
<i>T</i> , K	90.0(1)	110(1)	110(1)	90.0(1)	90.0(1)
max 2θ, deg	62.26	58.04	58.03	60.28	57.48
reflns, measd	66 603	50 440	18 715	34 453	72 390
unique reflns (<i>R</i> _{int} ^a)	16 399 (0.074)	14 187 (0.146)	13 269 (0.041)	15 864 (0.059)	12 655 (0.050)
reflns, <i>I</i> > 4σ(<i>I</i>)	10 989	6 851	5 717	9 011	8 929
params, refined	854	830	793	1058	911
<i>R</i> (<i>F</i> _o) ^b [<i>I</i> > 2σ(<i>I</i>)]	0.083	0.085	0.111	0.049	0.077
w <i>R</i> ₂ (<i>F</i> _o ²) ^c	0.268	0.242	0.333	0.113	0.235
GOF	1.115	0.976	1.048	0.892	1.058

$$^a R_{\text{int}} = \sum |F_o^2 - F_o^2(\text{mean})| / \sum [F_o^2]. \quad ^b R(F_o) = \{ \sum |F_o - F_c| \sum F_o \}. \quad ^c wR_2(F_o^2) = \{ \sum [w(F_o^2 - F_c^2)]^2 / \sum [w(F_o^2)] \}^{1/2}.$$

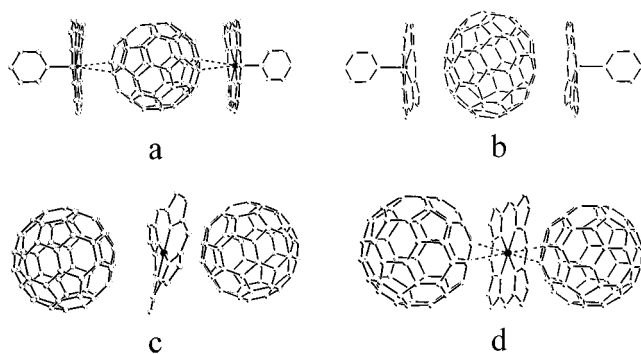


Figure 1. Different types of fullerene/porphyrin arrangement in 1–5: 2PyCoTPP·C₆₀·Cp₂Fe·C₇H₈ (**1**); (b) 2PyZnTPP·C₇₀·C₂HCl₃·C₇H₈ (**3**); (c) CoTMPP·C₆₀ (**4**); (d) CoTMPP·2C₆₀·3C₇H₈ (**5**). Phenyl groups of MTPP (M = Zn, Co) are not shown. Only one orientation of disordered C₇₀ molecule of two is shown for **3**.

Results

Synthesis. The preparation of fullerene complexes with porphyrins by evaporation of the solvent containing C₆₀ and corresponding metalloporphyrin in the presence of a large excess of Cp₂Fe (10-fold molar excess relative to fullerene) yields unexpected results as compared to the common procedure where no ferrocene was used.^{14,15} In some cases new phases of the ferrocene-containing complexes were formed quantitatively (**1**, **2**), while for **5** a solvent- and ferrocene-free complex, which is not formed without Cp₂Fe, has been obtained (see Experimental Section). These complexes are stable in air and do not lose solvent upon storage.

Molecular Packing and Order/Disorder of Fullerene Molecules in 1–5. Metalloporphyrin–fullerene arrangements in 1–5 are shown in Figure 1. **1** and **2** are isomorphous and isostructural, with fullerene and toluene molecules being on inversion centers and Cp₂Fe being located on a 2-fold axis (Figure 2a). The MTPP molecules in 1–3 lie in general positions. In **1**, C₆₀ molecules are ordered, whereas in **2** they are disordered over two orientations (70:30 occupancy ratio)

linked by noncrystallographic 2-fold axes. The C₆₀ moiety in **2** has 48 atomic positions common to both orientations, while disordered positions for the remaining 12 carbon atoms form a characteristic pattern of “crosses” on the fullerene sphere. Ferrocene molecules in **1** and **2**, determined with a relatively low precision due to disorder, as well as toluene and trichloroethylene solvate molecules in 1–3, show no shortened intermolecular contacts.

In **3**, which is generally isostructural to **1** and **2** notwithstanding a difference in the components, C₇₀ and toluene molecules are located on inversion centers. Strongly disordered trichloroethylene molecules are located on the 2-fold axes, like Cp₂Fe in **1** and **2** (Figure 2b). Since both C₇₀ and toluene molecules lack a center of symmetry, the disorder gives rise to two orientations with identical occupancy. Each isolated fullerene molecule in 1–3 is surrounded by the two PyMTPP moieties (where M = Co or Zn, Figure 2a,b). The shortest distances between the centers of the neighboring fullerene molecules are 13.7 Å in **1** and **2** and 14.0 Å in **3**.

The molecular packing in **4** (zigzag chains of C₆₀ spheres with van der Waals “caps” of CoTMPP) and in **5** (distorted honeycomb [C₆₀]_n layers with interspersed CoTMPP molecules, stacked with two neighboring fullerene moieties) is shown in Figures 3 and 4, respectively. The CoTMPP molecules stacked between two neighboring C₆₀ molecules occupy a general position in **4** and a center of symmetry in **5** (see Figure 1c,d), giving rise to 1:1 and 1:2 donor-to-fullerene ratio, respectively. The molecular packing in **5** is analogous to earlier studied benzene solvate of a C₆₀ complex with nonmetalated porphyrin H₂TPP·2C₆₀·4C₆H₆.¹⁵ The C₆₀ moiety is ordered in both CoTMPP complexes, with the shortest C₆₀···C₆₀ distances of 10.20 Å in **4** and 9.86 Å in **5** and the closest intermolecular C···C contacts of 3.68 Å (**4**) and 3.22 Å (**5**). A comparison with the C₆₀···C₆₀ distance of 9.94 Å in pure C₆₀²⁵ indicates a somewhat less dense arrangement of the molecules in **4**.

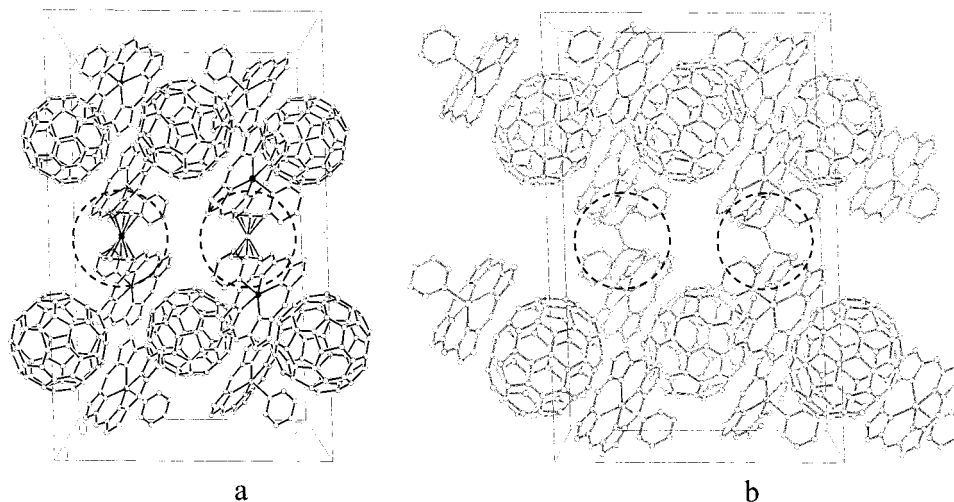


Figure 2. Molecular packing in the isomorphous $2\text{PyCoTPP}\cdot\text{C}_{60}\cdot\text{Cp}_2\text{Fe}\cdot\text{C}_7\text{H}_8$ (**1**) and $2\text{PyZnTPP}\cdot\text{C}_{60}\cdot\text{Cp}_2\text{Fe}\cdot\text{C}_7\text{H}_8$ (**2**) (a) and the isostructural $2\text{PyZnTPP}\cdot\text{C}_{70}\cdot\text{C}_2\text{HCl}_3\cdot\text{C}_7\text{H}_8$ (**3**) (b). Ferrocene molecules in **1** and **2** and trichloroethylene molecules in **3** are marked with dashed circles. Toluene molecule and phenyl groups of MTPP ($M = \text{Zn}, \text{Co}$) are not shown. Only one orientation of disordered C_{70} molecule of two is shown for **3**.

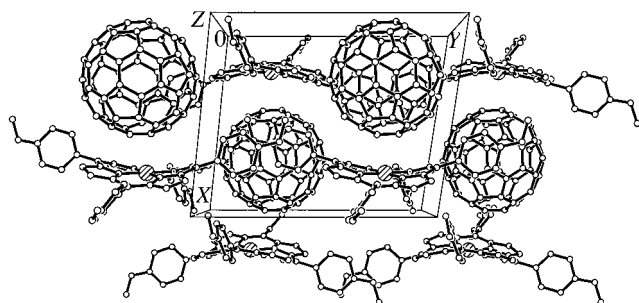


Figure 3. Molecular packing in $\text{CoTMPP}\cdot\text{C}_{60}$ (**4**).

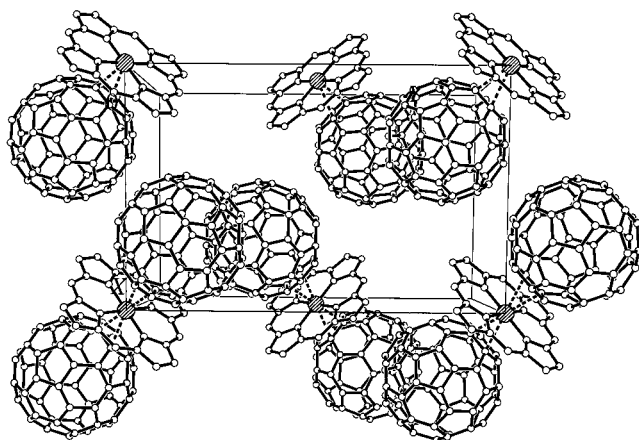


Figure 4. Molecular packing in $\text{CoTMPP}\cdot 2\text{C}_{60}\cdot 3\text{C}_7\text{H}_8$ (**5**); toluene molecules and *p*-methoxyphenyl groups of CoTMPP are not shown.

The closest intermolecular contacts of 3.35–3.45 Å between toluene molecules in **5** (an ordered one in a general position and a disordered one in the symmetry center) correspond to normal van der Waals interaction.

Structure of Metalloporphyrin Moieties. The main geometric parameters of porphyrin macrocyclic moieties (Figure 5) for **1–5** and related compounds^{26–29} are presented in Table 2. The values of bond lengths and angles in the

(25) Burgi, H.-B.; Blanc, E.; Schwarzenbach, D.; Liu, Shengzhong; Lu, Ying-jie; Kappes, M. M.; Ibers, J. A. *Angew. Chem., Int. Ed. Engl.* **1992**, *31*, 640.

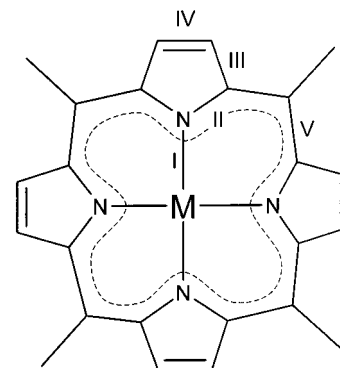


Figure 5. Notation of chemically equivalent bonds and bond angles in metalloporphyrin moiety for Table 2.

macrocyclic porphyrin ligand remain unchanged in **1–5** as compared to parent porphyrins. The cobalt atom in **1** is coordinated with pyridine and TPP in a flattened square-pyramidal manner, deviating by 0.190 Å from the mean plane of the macrocycle toward the Py ligand. In **2** and **3** the Zn atom deviates by ca. 0.43 Å out of the plane in the same direction. The Py ligand in **1–3** deviates by 5–8° from the normal to the porphyrin plane. It is interesting that the apical Co–N(Py) distance in **1** (2.154(2) Å) is close to the Zn–N(Py) distances in **2** and **3** (2.151(4) and 2.133(6) Å). The Co atoms in **4** and **5** have a square-planar coordination. The porphyrin ring in **4** has a saddlelike conformation, whereas in **5** it is planar within 0.04 Å. As shown in a review,³⁰ porphyrin nonplanarity may be caused, among other reasons, by the effect of an axial ligand and by steric effects. In **1–3** the square-pyramidal coordination of M atom corresponds well to that found in the related complex with tetra(4-pyridyl)porphyrin, PyZnTPyP .²⁷ The saddlelike geometry of

(26) Stevens, E. D. *J. Am. Chem. Soc.* **1981**, *103*, 5087.

(27) Collins, D. M.; Hoard, J. L. *J. Am. Chem. Soc.* **1970**, *92*, 3761.

(28) Hamor, M. J.; Hamor, T. A.; Hoard, J. L. *J. Am. Chem. Soc.* **1964**, *86*, 1938.

(29) Byrn, M. P.; Curtis, C. J.; Khan, S. I.; Sawin, P. A.; Tsurumi, R.; Strouse, C. E. *J. Am. Chem. Soc.* **1990**, *112*, 1865.

(30) Shelnutt, J. A.; Song, X.-Z.; Ma, J.-G.; Jia, S.-L.; Jentzen, W.; Medforth, C. J. *Chem. Soc. Rev.* **1998**, *27*, 31.

Table 2. Deviation of Metal Atom from Average Plane of Porphyrin Macrocycle (Δ), Selected Bond Distances and Bond Angles in Metalloporphyrin Moiety,^a and Metal–Fullerene Contacts in **1–5** and Related Compounds

porphyrin geom Δ (M), Å	1 planar 0.190	2 planar 0.435	3 planar 0.433	4 saddle 0.016	5 planar 0	CoTPP ²⁶ saddle 0	PyZnTPyP ^{b,27} planar 0.369	H ₂ TPP ²⁸ saddle	H ₂ TPP·2(<i>m</i> -xylene) ²⁹ planar
Bond Lengths, Å									
I	1.986(1)	2.072(2)	2.075(3)	1.937(1)	1.980(1)	1.948(1)	2.073(2)		
II	1.375(1)	1.377(2)	1.370(3)	1.380(1)	1.379(2)	1.378(1)	1.369(2)	1.350(5)	1.377(6)
III	1.438(1)	1.446(2)	1.443(3)	1.435(1)	1.437(2)	1.441(1)	1.446(2)	1.443(5)	1.431(6)
IV	1.348(2)	1.351(4)	1.349(5)	1.349(2)	1.352(3)	1.361(1)	1.356(3)	1.361(5)	1.354(8)
V	1.392(1)	1.401(2)	1.405(3)	1.392(1)	1.390(2)	1.390(1)	1.409(2)	1.403(5)	1.391(6)
Bond Angles, deg									
III	127.5(1)	126.6(1)	126.5(1)	127.2(1)	127.5(1)	127.4(2)	126.2(1)		
IIII	104.9(1)	106.4(2)	106.6(3)	105.4(1)	104.9(1)	105.1(2)	106.6(2)	108.8(4)	106.1(8)
IIIII	110.7(1)	109.6(1)	109.6(2)	110.1(1)	110.7(1)	110.8(2)	109.8(2)	108.7(3)	109.9(6)
IIIV	106.8(1)	107.2(2)	107.1(2)	107.2(1)	106.9(2)	106.6(2)	106.9(2)	106.9(4)	107.0(6)
IV	125.9(1)	125.5(2)	125.6(2)	125.0(1)	125.9(1)	125.6(2)	125.9(2)	126.0(4)	124.6(6)
VV	123.0(2)	125.8(2)	125.5(3)	121.8(1)	122.9(2)	121.9(2)	124.7(2)	125.1(5)	126.9(8)
M···C _n , Å	2.82–3.49	3.07–3.32	3.09–3.46	3.16–3.41	2.64–3.55				

^a For notations see Figure 5. ^b TPyP = tetra(4-pyridyl)porphyrin.

porphyrin moiety in **4** is induced by packing forces, as in many solvent- and fullerene-free molecular crystals, viz. CoTPP,²⁶ H₂TPP,²⁸ and other porphyrin derivatives.³⁰

Metalloporphyrin–Fullerene Contacts in 1–5. In the isostructural complexes **1–3** of C₆₀ and C₇₀ with PyMTPP, fullerene molecules arrange near the metal atoms at the apical site opposite the Py ligand. Slightly shortened Co···C(C₆₀) contacts in **1** (2.82 and 3.07 Å, Figure 1a) involve two carbon atoms of the 5–6 bond of C₆₀ which is almost parallel to the N–Co–N line in the CoTPP molecule. These contacts are close to the similar contacts found in fullerene complexes with CoOEP³⁴ (2.67–2.86 Å).¹³ Unlike **1**, all intermolecular contacts between PyZnTPP and fullerenes in **2** and **3** correspond to typical van der Waals distances, due to a stronger displacement of the zinc atom toward the pyridine ligand in the square-pyramidal coordination environment. The shortest Zn···C(fullerene) distance (3.08 Å) is longer than the corresponding distances in the C₆₀ complexes with ZnOEP³⁴ (2.94–2.98 Å)^{13,16} or the C₇₀ complex with ZnTPP (2.85–2.96 Å).¹⁴

All intermolecular Co···C(C₆₀) contacts in **4** have typical van der Waals lengths. The two C₆₀ molecules above and below porphyrin moiety are located asymmetrically relative to saddlelike CoTMPP. The shortest Co···C(C₆₀) distances are 3.17 and 3.26 Å with the 6–5 bond of the “A” C₆₀ molecule and 3.40 and 3.68 Å with the 6–6 bond of the “B” C₆₀ molecule (Figure 1c).

Unlike **4**, the planar CoTMPP molecule in **5** forms distinctly short Co···C(C₆₀) contacts (2.65 and 2.67 Å) with the two C₆₀ molecules located symmetrically above and below the porphyrin plane (Figure 1d). These short contacts complement a square-planar coordination of the Co atom in CoTMPP to give a square-bipyramidal arrangement with the centers of the 6–6 bonds of the two neighboring C₆₀ molecules in apical positions. As in **1**, the weakly coordinating C–C bonds of fullerene moieties are parallel to the N–Co–N line in the CoTMPP molecules.

IR Spectra. The IR spectra of the complexes are a superposition of those of the individual components, namely

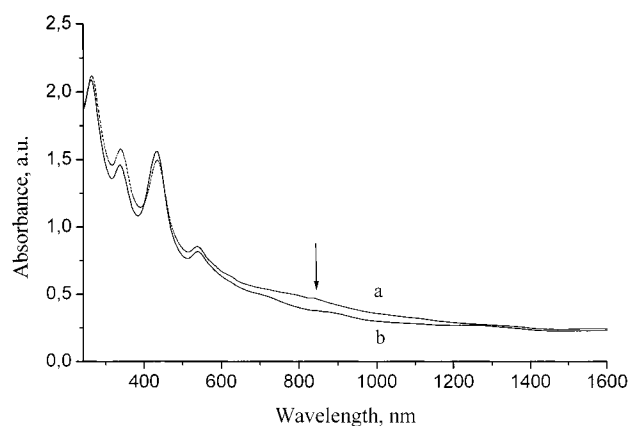


Figure 6. UV–visible absorption spectra of CoTMPP·2C₆₀·3C₇H₈ (**5**) and CoTMPP·C₆₀ (**4**) in KBr matrix. The arrow shows the position of the CT band.

C₆₀ or C₇₀ and metal tetraarylporphyrins. The spectra of **1** and **2** also show the bands ascribed to Cp₂Fe.

The bands of the F_{1u}(4) vibration of C₆₀ are observed at 1427 cm⁻¹ for **1** and **2** and at 1429 cm⁻¹ for **4** and **5** as compared to that of parent fullerene at 1429 cm⁻¹. However, the absorption bands of metalloporphyrins in **1–5** are slightly shifted (up to 8 cm⁻¹). The position of the Cp₂Fe bands in **1** and **2** coincides with that for pure Cp₂Fe.

UV–Visible Spectra. The UV–visible spectra of **1–5** are also a superposition of the spectra of the starting compounds. The spectra of the C₆₀ complexes with CoTMPP (**4** and **5**) are shown in Figure 6. The bands at 262 and 339 nm (**4**) and 261 and 336 nm (**5**) are ascribed to C₆₀. These bands are blue shifted up to 8 nm relative to those of parent C₆₀ (266 and 344 nm). The bands at 433 and 537 nm in **4** and **5** are attributed to the CoTMPP chromophore (Figure 6a,b). These bands are red shifted by up to 7 nm relative to those of starting CoTMPP (426 and 536 nm). The bands of ZnTPP and CoTPP in the pyridine-containing complexes (**1–3**) show larger red shifts (up to 15 nm) relative to parent metalloporphyrin.

Additional weak absorption in the visible range with a maximum at 830 nm in **5** may be evidence of charge transfer from CoTMPP to the C₆₀ molecule (Figure 6a).

Discussion

IR and UV–Visible Spectra. Molecular complexes **1–5** differ by their donor-to-fullerene ratio, viz. 2:1 in **1–3** (with the additional donor component Cp_2Fe in **1** and **2**, and solvent molecules in all cases), 1:1 in **4**, and 1:2 in **5**.

The IR data (see Results) show only small shifts (up to 2 cm^{-1}) of the $\text{F}_{1u}(4)$ vibration, which is the most sensitive to charge transfer to the C_{60} molecule,³¹ providing strong evidence for the fully van der Waals character of the complexes. The shifts of the bands of metalloporphyrin molecules observed in **1–5** seem to be associated with changes in geometry rather than with charge transfer.

On the formation of **4** and **5**, noticeable shifts of both C_{60} and CoTMPP bands are observed in the UV–visible spectra. The shifts observed earlier in the spectra of other fullerene complexes with metal tetraphenylporphyrins¹⁵ may be associated with the interaction of C_{60} and CoTMPP π -systems. Larger red shifts of the CoTPP and ZnTPP bands in **1–3** are attributed to additional coordination of pyridine to the central metal cation of porphyrin. The intensity of charge transfer bands depends on the efficiency of HOMO–LUMO overlapping between donor and acceptor molecules. Actually the charge transfer band is observed only in the spectrum of **5** in which the distances between the porphyrin and C_{60} molecules are the smallest among **1–5**.

Molecular packing and weak intermolecular interactions in **1–5** together with a detailed analysis of these factors will be discussed below for all published molecular complexes of fullerenes with porphyrin counterparts.

Packing and Intermolecular Interactions in 1–5. A dense packing principle³² applied to molecular complexes of fullerenes with porphyrins requires a close arrangement of their spheroid and disklike molecules with little or no voids in between. Filling the cavities that inevitably exist between such moieties requires either smaller molecules of solvent and/or second donor counterpart, or conformational flexibility of a porphyrin moiety. Both variants are observed in the complexes under discussion, viz. filling intermolecular cavities (**1–3**, **5**) and saddlelike conformation of CoTMPP in the solvent-free **4**. Similar saddlelike geometry was observed earlier in solvent-free porphyrin crystals (see Table 2), whereas $\text{H}_2\text{TPP}\cdot\text{C}_{60}\cdot 3\text{C}_7\text{H}_8$, $\text{H}_2\text{TPP}\cdot 2\text{C}_{60}\cdot 3\text{C}_6\text{H}_6$, $\text{H}_2\text{TPP}\cdot 2\text{C}_{60}\cdot 4\text{C}_6\text{H}_6$, and $\text{CuTPP}\cdot\text{C}_{70}\cdot 1.5\text{C}_7\text{H}_8\cdot 0.5\text{C}_2\text{HCl}_3$ prepared earlier¹⁵ contain almost planar porphyrin molecules and from one to three solvent molecules per fullerene moiety.

The metalloporphyrin–fullerene frameworks in **1**, **2**, and **3** have two types of cavities, occupied by different guest molecules (Figure 1a,b). The cavities of the first type are of similar size and are occupied by toluene molecules (which can be described as elongated disks with dimensions of ca. $7.5 \times 7 \times 3.5\text{ \AA}$). The cavities of the second type are larger in **1** and **2** than in **3** because of a smaller size of the C_{60} sphere relative to the C_{70} ellipsoid. As a result, the cavity of the second type in **3** is occupied only by trichloroethylene

molecule (distorted squares with diagonals of ca. $7.5 \times 6\text{ \AA}$ and a thickness of ca. 3.4 \AA), whereas in **1** and **2** the cavity is large enough to accommodate a bulkier ferrocene molecule (almost spherical with a diameter of ca. 6.8 \AA).

The lack of short van der Waals contacts of guest molecules in **1–3** is indicative of their “loose” positioning in the porphyrin–fullerene framework. Such an unconstrained van der Waals environment gives rise to disorder observed for all guest components, including ferrocene (see Experimental Section). Parallel sandwich conformations of the Cp_2Fe moieties in **1** and **2** are similar to those of pure ferrocene³³ or the ferrocene molecule in $2\text{Cp}_2\text{Fe}\cdot\text{C}_{60}$.¹¹

The difference in the $\text{Co}\cdots\text{C}_{60}$ (in **1**) and $\text{Zn}\cdots\text{C}(\text{C}_{60})$ (in **2**) distances may be associated with a stronger metal– C_{60} $d-\pi$ interaction in the case of cobalt. The shortened $\text{Co}\cdots\text{C}(\text{C}_{60})$ distances in **1** are accompanied by the ordering of the C_{60} molecules (see Figure 1a), while the absence of any secondary bonding between zinc atoms and fullerenes in **2** and **3** results in rotational disorder in the fullerene molecules in these complexes (Figure 1b). However, no substantial changes are observed in the spectra of **1**. Thus, higher ordering may also be a result of better van der Waals fitting of C_{60} to MTPP in the Co complex with more flattened CoTPP environment.

Crystal Structures and Packing in Known Fullerene–Porphyrin Complexes. Molecular complexes of fullerenes with porphyrins and metalloporphyrins as a donor component (D), studied by single-crystal X-ray diffraction, are summarized in Table 3. The main supramolecular characteristics, defining their composition and properties, are the motif of fullerene–donor packing and cavities therein, conformation of the porphyrin macrocycle, shortest intermolecular contacts of fullerene–porphyrin, and fullerene–fullerene distances. Special attention is paid here to the existence, or absence, of disorder of the fullerene molecules, shortest metal–fullerene distances, and the conformation of a macrocycle.

As a convenient tool which readily reveals errors in reported composition and/or crystal structures, the *packing coefficient* k ³² has been calculated for each compound. This parameter, defined commonly as a fraction of the unit cell volume occupied by molecules, usually attains 0.70–0.78 in molecular crystals. Thus, an unreasonably high value of packing coefficient $k = 1.11$ for the reported complex

- (33) (a) Seiler, P.; Dunitz, J. D. *Acta Crystallogr., Sect. B* **1979**, *35*, 1068. (b) Seiler, P.; Dunitz, J. D. *Acta Crystallogr., Sect. B* **1979**, *35*, 2020. (c) Seiler, P.; Dunitz, J. D. *Acta Crystallogr., Sect. B* **1982**, *38*, 1741.
- (34) Donor compounds and their abbreviations: H_2TPP , 5,10,15,20-tetra-phenyl-21*H*,23*H*-porphyrin; ZnTPP, zinc 2,3,7,8,12,13,17,18-octaethyl-21*H*,23*H*-porphyrinate; CoTPP, cobalt(II) 5,10,15,20-tetra-phenyl-21*H*,23*H*-porphyrinate; CuTPP, copper(II) 5,10,15,20-tetra-phenyl-21*H*,23*H*-porphyrinate; CoTMPP, cobalt(II) 5,10,15,20-tetrakis(*p*-methoxyphenyl)-21*H*,23*H*-porphyrinate; CoOEP, cobalt(II) 3,7,8,12,13,17,18-octaethyl-21*H*,23*H*-porphyrinate; ZnOEP, zinc 2,3,7,8,12,13,17,18-octaethyl-21*H*,23*H*-porphyrinate; ET (BEDT-TTF), bis(ethylenedithio)-tetrathiafulvalene; Cp_2Fe , ferrocene; Py, pyridine; TMDTDM-TTF, tetramethylenedithio-4,5-dimethyltetrathiafulvalene; DBTTF, dibenzotetrathiafulvalene; TPDP, 3,3',5,5'-tetraphenyldipyranilidene; TP, triphenylene; DPA, 9,10-diphenylanthracene.
- (35) Everywhere in this paper, we refer to the potential donor components in the neutral molecular complexes, capable of forming cations under oxidation, as “donor molecules”.

(31) Picher, T.; Winkler, R.; Kuzmany, H. *Phys. Rev. B* **1994**, *49*, 15879.

(32) Kitaigorodskii, A. I. *Organic Crystal Chemistry*; Consultants Bureau: New York, 1957; p 106.

Table 3. Molecular Complexes of Fullerenes/Porphyrins with Known Crystal Structures^a

macrocyclic donors (D) ^b	C _n	ratio D/C _n	solvent ^c	C _n order	M···C (center···C)	conformation of D	k	packing motif according to Figure 7	ref
H ₂ TPP	C ₆₀	1/2	1.5C ₆ H ₆	–	(2.77, 2.86)	P	0.73	framework [2C ₆₀ ·D] _n , with channels	15
H ₂ TPP	C ₆₀	1/2	2C ₆ H ₆	–	(2.67, 2.78)	P	0.74	puckered honeycombs [C ₆₀] _n , D in between	15
H ₂ TdMePP	C ₆₀	2/3	1.33C ₇ H ₈	–	n/a	P	0.73	zigzag chains [C ₆₀ ·D] _n + isolated C ₆₀	14
H ₂ TPP	C ₆₀	1	3C ₇ H ₈	–	(2.70, 2.75)	P	0.75	contacting zigzag chains [C ₆₀ ·D] _n	14
H ₂ TdBuPP	C ₆₀	1	–	–	(2.69, 2.88)	P	0.68	zigzag chains [C ₆₀ ·D] _n	14
H ₂ TpivPP	C ₆₀	1	–	–	n/a	S	0.71	n/a	14
H ₂ TdMePP	C ₇₀	1	4C ₇ H ₈	–	(2.86)	P	0.73	linear chains [C ₇₀ ·D] _n	14
NiTMPP	C ₇₀	1/2	1C ₇ H ₈	–	2.99, 3.04	P	0.75	n/a	14
CoTMPP	C ₆₀	1/2	1.5C ₇ H ₈	+	2.65, 2.67	P	0.75	puckered honeycombs [C ₆₀] _n , D in between	this work ^d
CoTMPP	C ₆₀	1	–	+	3.17, 3.26	S	0.77	zigzag chains [C ₆₀] _n , D in between	this work ^e
CuTPP	C ₆₀	2	–	–	3.42	S	0.77	linear chains [C ₆₀] _n , (D) ₂ pairs	15
CuTPP	C ₇₀	1	1.5C ₇ H ₈ , 0.5C ₂ HCl ₃	+	2.88, 2.90	P	0.71	zigzag chains [C ₇₀] _n , D in between	15
ZnTPP	C ₇₀	1	–	+	2.89	P	0.61	as above	14
FeTPP ⁺ B(C ₆ F ₅) ₄ [–]	C ₆₀	1	2.5C ₆ H ₄ Cl ₂	–	2.63, 3.11	S	0.73	zigzag chains [C ₆₀] _n , capping D in between	17
ClFeOEP	C ₆₀	1	1CHCl ₃	–	3.20	P	0.74	as above	13
PyCoTPP	C ₆₀	2	1C ₇ H ₈ , 1Cp ₂ Fe	+	2.82, 3.07	P	0.73	isolated D·C ₆₀ ·D groups	this work ^f
PyZnTPP	C ₆₀	2	1C ₇ H ₈ , 1Cp ₂ Fe	–	3.08	P	0.72	as above	this work ^g
PyZnTPP	C ₇₀	2	1C ₇ H ₈ , 1C ₂ HCl ₃	–	3.08	P	0.70	as above	this work ^h
CoOEP	C ₆₀	2	1CHCl ₃	+	2.67, 2.78	P	0.74	helices [C ₆₀ ·2D] _n	13
CoOEP	C ₆₀ O	2	1CHCl ₃	+	2.67, 2.73	P	0.75	as above	13
ZnOEP	C ₆₀	2	1CHCl ₃	+	2.94, 2.98	P	0.75	as above	13
ZnOEP	C ₆₀	2	2C ₆ H ₆	–	2.98	P	0.75	as above	13
CoOEP	(C ₆₀) ₂ O	1	0.4C ₆ H ₆ , 0.6CHCl ₃	–	2.67	P	1.11	n/a	13
		1/2					0.74		
CoOEP	C ₇₀	1	1C ₆ H ₆ , 1CHCl ₃	+	2.80	P	0.77	zigzag chains [C ₇₀] _n , capping pairs (D) ₂ in between	13
NiOEP	C ₇₀	1	1C ₆ H ₆ , 1CHCl ₃	+	2.83	P	0.76	as above	13
CuOEP	C ₇₀	1	1C ₆ H ₆ , 1CHCl ₃	+	2.92	P	0.77	as above	13
CuOEP	C ₆₀	1	2C ₆ H ₆	+	3.02	P	0.76	puckered honeycombs [C ₆₀] _n , pairs D ₂ in between	16
PdOEP	C ₆₀	1	1.5C ₆ H ₆	+	3.04, 3.08	P	0.74	as above	16
Ru(CO)(OEP)	C ₆₀	1	2C ₇ H ₈	–	2.83	P	0.75	zigzag chains [C ₆₀] _n , capping D in between	16
CoOEP	Sc ₃ N@C ₈₀	1	0.5C ₆ H ₆ , 1.5CHCl ₃	–	2.79	P	0.76	zigzag chains [M ₃ N@C ₇₀] _n , capping pairs (D) ₂ in between	18a
CoOEP	ErSc ₂ N@C ₈₀	1	1.5C ₆ H ₆ , 0.3CHCl ₃	–	2.71, 2.75	P	0.76	as above	18b
CoOEP	Sc ₃ N@C ₇₈	1	1.5C ₆ H ₆ , 0.3CHCl ₃	–	–	P	0.76	as above	18c

^a Unusually low and high packing densities are in italics; suggested correct values are in bold type. ^b H₂TdMePP, tetra(3,5-dimethylphenyl)porphyrin; H₂TdBuPP, tetra(3,5-di-*tert*-butylphenyl)porphyrin; H₂TpivPP, tetra(2-pivaloylphenyl)porphyrin; NiTMPP, nickel tetra(*p*-methylphenyl)porphyrinate; MOEP, metal octaethylporphyrinate; P, parallel conformation; S, saddle conformation; k, packing coefficient. ^c Per one fullerene molecule. ^d Compound 5. ^e Compound 4. ^f Compound 1. ^g Compound 2. ^h Compound 3.

(C₆₀)₂O·CoOEP·0.4C₆H₆·0.6CHCl₃¹³ most likely indicates a misprint, whereas the tentative composition (C₆₀)₂O·2CoOEP·0.4C₆H₆·0.6CHCl₃, with Z = 2 instead of Z = 4, gives the normal value of k = 0.74. Other outlying values of k in the reported solvent-free complexes, viz. H₂TdBuPP·C₆₀ (k = 0.68)¹⁴ and ZnTPP·C₇₀ (k = 0.61),¹⁴ may be indicative of the presence of some disordered solvent molecules, not revealed in the original X-ray studies. This is very likely the case for the latter compound, due to its isomorphism with CuTPP·C₇₀·1.5C₇H₈·0.5C₂HCl₃¹⁵ (see below).

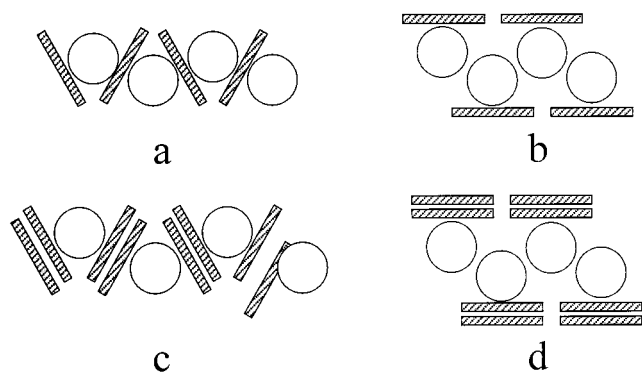
The porphyrin–fullerene ratio in the structurally studied complexes of C₆₀, C₇₀, and M₃N@C₈₀ vary from 1:2 to 2:1. In all complexes, little or no ground-state charge transfer from donor to fullerene has been reported.^{13–18} The planar conformation of the porphyrin macrocycle clearly predominates, although the porphyrin molecules attain a saddlelike conformation, fitting the convex C_n moieties in solvent-free H₂TpivPP·C₆₀,¹⁴ 2CuTPP·C₆₀,¹⁵ and CoTMPP·C₆₀ (**4**). The predominance of planar macrocycle conformation probably has its origin in packing forces, as a survey of Cambridge

Structure Database (CSD) data for pure porphyrins and their (fullerene-free) solvates showed saddle and planar conformations to be almost equally favorable. Raston and co-workers²⁰ studied a series of related supramolecular fullerene complexes with substituted tetraazo-macrocylic derivatives of 3d metals, in which a saddle conformation of the macrocyclic moiety is forced by intramolecular steric repulsion.

The most common packing motifs in molecular complexes with 1:2 and 1:1 porphyrin-to-fullerene ratios are zigzag chains of alternating fullerene and donor molecules, the latter being sandwiched between fullerenes (Figure 7a). A few other arrangements, such as linear chains [D–C₇₀–D–C₇₀]_n in H₂TdMePP·C₇₀·4C₇H₈ and zigzag chains [D–C₆₀–D–C₆₀]_n with the symmetrically independent isolated C₆₀ moieties in 2H₂TdMePP·3C₆₀·4C₇H₈, were observed.¹⁴ However, more interfullerene contacts, which give rise to chains and frameworks of C_n, may also exist in fullerene-rich compositions with D:C_n ratios of 1:2 and 2:3. A complementary motif in 1:1 complexes consists of zigzag chains of fullerene moieties with “capping” porphyrins (Figure 7b),

Table 4. Series of Isomorphous Porphyrin/Fullerene Complexes

	$\text{H}_2\text{TPP}\cdot 2\text{C}_{60}\cdot 4\text{C}_6\text{H}_6$	$\text{CoTMPP}\cdot 2\text{C}_{60}\cdot 3\text{C}_7\text{H}_8$	$\text{H}_2\text{TPP}\cdot \text{C}_{60}\cdot 3\text{C}_7\text{H}_8$	$\text{CuTPP}\cdot \text{C}_{70}\cdot 1.5\text{C}_7\text{H}_8\cdot 0.5\text{C}_2\text{HCl}_3$	$\text{ZnTPP}\cdot \text{C}_{70}$	$2\text{PyCoTPP}\cdot \text{C}_{60}\cdot \text{Cp}_2\text{Fe}\cdot \text{C}_7\text{H}_8$	$(\text{PyZnTPP})_2\text{C}_{60}\cdot \text{p}_2\text{Fe}\cdot \text{C}_7\text{H}_8$	$(\text{PyZnTPP})_2\text{C}_{70}\cdot \text{C}_7\text{H}_8\cdot \text{C}_2\text{HCl}_3$
system	monoclinic	monoclinic	triclinic	triclinic	triclinic	monoclinic	monoclinic	monoclinic
<i>a</i> , Å	13.7422(6)	13.984(1)	14.2783(3)	14.3756(6)	14.4805(1)	30.5233(4)	30.797(2)	30.763(3)
<i>b</i> , Å	20.765(1)	21.388(2)	16.7220(3)	16.5497(8)	16.5025(2)	19.5925(2)	19.532(2)	19.825(2)
<i>c</i> , Å	18.626(1)	18.178(2)	17.0596(3)	17.6590(9)	17.7287(3)	19.2515(2)	19.312(1)	20.036(2)
α , deg	90	90	69.115(1)	72.460(1)	72.623(1)	90	90	90
β , deg	91.814(4)	96.586(2)	85.338(1)	86.278(1)	86.580(1)	92.067(1)	91.861(2)	92.250(2)
γ , deg	90	90	78.164(1)	80.577(1)	80.574(1)	90	90	90
<i>V</i> , Å ³	5312	5401	3725	3951	3988	11505	11611	12210
space group	<i>P</i> 2 ₁ / <i>c</i>	<i>P</i> 2 ₁ / <i>c</i>	<i>P</i> 1̄	<i>P</i> 1̄	<i>P</i> 1̄	<i>C</i> 2/ <i>c</i>	<i>C</i> 2/ <i>c</i>	<i>C</i> 2/ <i>c</i>
<i>Z</i>	4	4	2	2	2	4	4	4
ρ_{calc}	1.481	1.538	1.437	1.445	1.260	1.433	1.434	1.400
<i>k</i>	0.74	0.75	0.76	0.71	0.61	0.73	0.72	0.69

**Figure 7.** Schematic representation of different types of molecular arrangement in fullerene/porphyrin complexes. The explanations are given in the text.

which may be just another view on the same structure with both $\text{C}_n\cdots\text{D}$ and $\text{C}_n\cdots\text{C}_n$ short contacts. For porphyrin-rich complexes with a 2:1 composition, pairs of donor molecules may exist in either $[\text{C}_n\text{---D---D---C}_n]$ chains (Figure 7c) or zigzag fullerene chains with double porphyrin caps (Figure 7d). The isolated supramolecular grouping $\text{D}\cdot\text{C}_n\cdot\text{D}$ that exists in the first packing type is observed also in our 2:1 complexes **1–3**, in which a donor moiety with the axial Py ligand is not planar.

Isomorphous porphyrin–fullerene complexes were reported for $2\text{MOEP}\cdot\text{C}_{60}\cdot\text{CHCl}_3$ (where $\text{M} = \text{Co}, \text{Zn}$),¹³ $\text{MOEP}\cdot\text{C}_{70}\cdot\text{C}_6\text{H}_6\cdot\text{CHCl}_3$ (where $\text{M} = \text{Co}, \text{Ni}, \text{Cu}$),¹³ and the endohedral derivatives $\text{CoOEP}\cdot(\text{M}_3\text{N}@C_{80})\cdot\text{solv}$ (where $\text{M} = \text{Sc}, \text{Er}$),¹⁸ as well as complexes **1** and **2** in this paper (Table 1). The first series may be extended with the complex $2\text{ZnOEP}\cdot\text{C}_{60}\cdot 2\text{C}_6\text{H}_6$.¹⁶ The other three complexes of C_{60} with MOEP (1:1), where $\text{M} = \text{Cu}$ and Pd ,¹⁶ are also isomorphous. However, a broader term of *quasi-isomorphism* can be used in this class of compounds, in which crystals have close unit cell parameters but more variable content. Three families of quasi-isomorphous structures displayed in Table 4 include the monoclinic complexes **1–3** (see Results), the pair of monoclinic $\text{H}_2\text{TPP}\cdot 2\text{C}_{60}\cdot 4\text{C}_6\text{H}_6$ and $\text{CoTMPP}\cdot 2\text{C}_{60}\cdot 3\text{C}_7\text{H}_8$, and the triclinic crystals of $\text{H}_2\text{TPP}\cdot \text{C}_{60}\cdot 3\text{C}_7\text{H}_8$,¹⁴ $\text{CuTPP}\cdot \text{C}_{70}\cdot 1.5\text{C}_7\text{H}_8\cdot 0.5\text{C}_2\text{HCl}_3$,¹⁵ and $\text{ZnTPP}\cdot \text{C}_{70}$.¹⁴ Calculated density of $1.260\text{ g}\cdot\text{cm}^{-3}$ for $\text{ZnTPP}\cdot \text{C}_{70}$ deviates drastically from two other compounds of this family (1.437 and $1.445\text{ g}\cdot\text{cm}^{-3}$, respectively), which provides an additional argument for the presence of disordered solvent molecules in this crystal.

The shortened $\text{M}\cdots\text{C}(\text{fullerene})$ contacts in the range of

$2.6\text{--}3.0\text{ \AA}$ are observed in a number of complexes listed in Table 3. Although the distances from the fullerene carbon atoms to the (empty) center of the neighboring macrocycle in H_2TPP and related metal-free porphyrins have similar values, the shortened metal–fullerene contacts clearly correlate to the orientational ordering of the C_{60} and C_{70} molecules (see isomorphous **1** and **2**). The use of metalloporphyrins as disorder-hindering agents in mixed fullerene crystals is therefore justified. However, this is not so clear for molecular complexes of endohedral metallofullerenes, for which the metal moiety may itself be disordered within the carbon shell.¹⁸ In some cases even in the presence of the shortened $\text{C}\cdots\text{M}$ contacts the C_n moiety is disordered, as in $\text{Ru}(\text{CO})\text{OEP}\cdot\text{C}_{60}\cdot 2\text{C}_7\text{H}_8$.¹⁶ A family of quasi-isomorphous crystals with similar molecular packing may include both ordered metal-containing and disordered metal-free porphyrin complexes of fullerenes (see Table 4). A specific $\text{M}\cdots\text{C}_n$ interaction therefore does not determine the supramolecular arrangement of the complex as a whole, although it can bring more ordering in favorable cases.

Conclusion

The study of the formation of fullerene complexes with metal tetraarylporphyrins in the presence of ferrocene illustrates synthetic possibilities of this method in preparing both solvated multicomponent and solvent-free phases. In the fullerene complexes with planar porphyrin molecules, the vacancies can be occupied not only by solvent molecules but also by other donor ones. The multicomponent complexes $\text{D}_1\cdot\text{D}_2\cdot\text{C}_{60}\cdot\text{S}_i$ (where D_1 is a structure-forming molecule and D_2 is another donor molecule) obtained by this procedure have potential for modification of their physical properties (by changing D_2), while retaining the crystal structure of the compound (preserving the same D_1). Using D_2 molecules with strong donor properties, one can change electronic characteristics of the complexes.

The information on fullerene complexes with porphyrins obtained so far shows great advantages of porphyrins as compared to other organic π -donors in the design of functional fullerene-based molecular solids. The complexes have a great variety of packing motifs (from a three-dimensional framework to isolated packing of fullerenes) and conformational flexibility of porphyrin counterparts. Weak secondary $\text{M}\cdots\text{C}(\text{fullerene})$ binding may prevent rotation of fullerene molecules in favorable packing motifs. The pres-

ence of large vacancies or channels between planar porphyrin molecules and spherical fullerenes allows incorporation of other donor molecules into a complex.

Acknowledgment. The work was supported by the Linkage Grant of NATO Science Program, the Russian Program “Fullerenes and Atomic Clusters”, Presidium of Russian Academy of Sciences (Young Scientists’ Projects program), Russian Foundation for Basic Research (Grants

99-03-32810 and 00-03-32577a), and the National Science Foundation (CHE9981864).

Supporting Information Available: IR and UV–vis–NIR spectroscopic data; five X-ray crystallographic files in CIF format. This material is available free of charge via the Internet at <http://pubs.acs.org>.

IC011312L